

# Ferroelectric phase transition, ionicity condensation, and multicriticality in charge transfer organic complexes

Jun-ichiro Kishine,<sup>a\*</sup> Tadeusz Luty,<sup>b</sup> and Kenji Yonemitsu,<sup>a</sup>

<sup>a</sup> *Department of Theoretical Studies,  
Institute for Molecular Science, Okazaki 444-8585, Japan*  
and

*Department of Functional Molecular Science,  
Graduate University for Advanced Studies,  
Okazaki 444-8585, Japan*

<sup>b</sup> *Institute of Physical and Theoretical Chemistry Technical University of Wroclaw 50-370 Wroclaw, Poland*

(Dated: June 7, 2018)

To elucidate a novel pressure-temperature phase diagram of the quasi-one-dimensional mixed-stack charge-transfer (CT) complex TTF-CA, we study the quasi-one-dimensional spin-1 Blume-Emery-Griffith (BEG) model. In addition to the local charge transfer energy and the inter-stack polar (dipole-dipole) interaction, we take account of the inter-stack electrostriction effect. Using the self-consistent chain-mean-field theory, where the intra-stack degrees of freedom are exactly treated by the transfer-matrix method, we reproduce the gas-liquid-solid like phase diagram corresponding to the neutral (N), paraelectric ionic ( $I_{\text{para}}$ ), and ferroelectric ionic ( $I_{\text{ferro}}$ ) phases, respectively. We also give an explanation on the experimentally observed multicritical behavior and concomitant discontinuous inter-stack lattice contraction in TTF-CA.

PACS numbers:

## I. INTRODUCTOIN

In the “critical phase control technology,” condensed molecular materials play quite a promising role, because molecular orbitals and stacking architecture are manipulable in a desirable way. To elucidate interrelation of constituent molecular structures and emergence of various thermodynamic phases such as superconductivity, magnetism, and ferroelectricity is of great interest there. A neutral-to-ionic phase transition (NIT) in quasi-one-dimensional charge-transfer (CT) complexes comprising mixed-stack architecture of electron donor (D) and acceptor (A) molecules<sup>1</sup> has played a key role in this field.

In particular, phase control by pressure<sup>2,3</sup> or laser radiation<sup>3,4</sup> in the tetrathiafulvalene-*p*-chloranil (TTF-CA), that exhibits the NIT around 80K at ambient pressure, has attracted a great deal of interest. Very recently, Collet *et al.*,<sup>5</sup> using highly refined time-resolved X-ray diffraction technique, have reported direct observation of a photo-induced paraelectric-to-ferroelectric structural order in the crystal. In the ionic phase, the  $D^+A^-$  pair forms a dimer due to the electrostatic instability<sup>6</sup> or subsequent spin-Peierls instability.<sup>7</sup> The ionized dimer on the DA chain carries a local electric dipole moment  $p$  with opposite directions depending on the dimerization patterns  $\underline{D^+A^-}$  or  $\underline{A^-D^+}$ . Once  $p$  acquires a macroscopic mean value  $\eta = \langle p \rangle \neq 0$ , a spontaneous inversion symmetry breaking (SISB) occurs and the system undergoes a phase transition to a ferroelectric-ionic ( $I_{\text{ferro}}$ ) phase.

The ionic phase itself is simply described by ionicity condensation  $c = \langle p^2 \rangle \sim 1$ . Since  $\eta$  is a symmetry-breaking order parameter but  $c$  is not, we expect that  $\eta$  and  $c$  play separate roles. The appearance of two distinct order parameters  $\eta$  and  $c$  is a direct consequence of the degeneracy of the two configurations of dimerization pattern, IA ( $\dots \underline{D^+A^-} \underline{D^+A^-} \dots$ ) and ( $\dots \underline{A^-D^+} \underline{A^-D^+} \dots$ ).

Recently, the respective roles of  $c$  and  $\eta$  have been highlighted in both equilibrium<sup>2</sup> and nonequilibrium<sup>3</sup> processes. Using the neutron diffraction along with nuclear-quadrupole-resonance (NQR) measurements, Lemée-Cailleau *et al.*<sup>2</sup> found a novel phase where *the system is ionic but dipoles remain disordered*, i.e., a paraelectric ionic ( $I_{\text{para}}$ ) phase. They proposed a pressure-temperature phase diagram of TTF-CA, where the N,  $I_{\text{para}}$ , and  $I_{\text{ferro}}$  phases are like gas, liquid, and solid phases, respectively. The ferroelectric order is well signaled by the appearance of  $(0, 2k+1, 0)$  Bragg peaks that indicate the inversion symmetry breaking. The “sublimation” line separating the N and  $I_{\text{ferro}}$  phases continues up to a triple point  $(P_t, T_t) \sim (500\text{MPa}, 210\text{K})$ . Above the triple point, in addition to the “crystallization (or melting)” line, there appears a “condensation” line separating the  $I_{\text{para}}$  and  $I_{\text{ferro}}$  phases accompanied by a concomitant discontinuous change of  $c$ , ending at a critical point  $(P_c, T_c) \sim (700\text{MPa}, 250\text{K})$ . The purpose of this paper is to give a qualitative understanding of this phase diagram. This phase diagram, in addition to the phenomenological description offered in ref.<sup>3</sup>.

Since the SISB is prohibited by thermal fluctuations in a purely one-dimensional stack, inter-stack coupling is required to realize the SISB. In addition, the experimental observation strongly indicates that electronic and lattice degrees of freedom are coupled with each other in a unique manner. That is to say, upon crossing the tran-

\*Address after September 2003: *Department of Physics, Faculty of Engineering, Kyushu Institute of Technology, 1-1 Sensuicho, Tobata, Kitakyushu 804-8550, Japan*

sition lines in the gas-liquid-solid like phase diagram,<sup>2,3</sup> the unit cell parameter  $b$  (for the axis perpendicular to the stack) exhibits about 0.5 % discontinuous contraction at the condensation transition but exhibits continuous contraction at the crystallization transition. On the other hand, the unit cell parameter  $a$  (for the stacking axis) exhibits only continuous contraction at the condensation transition and below it remains almost constant.<sup>3</sup> Now we are ready to ask the question: (1) what kind of inter-stack interactions are responsible for the occurrence of the  $I_{\text{ferro}}$  phase, and (2) how the lattice anomalies are coupled to the phase transitions?

As for the first question, Luty *et al.*<sup>3,8</sup> stressed that the inter-stack non-polar coupling<sup>7</sup> alone cannot drive the ferroelectric ordering and the *dipolar* coupling plays an essential role. As for the second question, Kawamoto *et al.*<sup>9</sup> took account of the charge distribution on the atoms inside each molecule by an ab initio quantum chemical method and elucidated the importance of inter-stack Coulomb attraction  $\sim -0.14\text{eV}$ , which may cause inter-stack electrostriction (Coulomb-lattice coupling).

## II. QUASI-ONE-DIMENSIONAL BLUME-EMERY-GRIFFITH MODEL AND INTERCHAIN MEAN FIELD THEORY

Now we shall set up a model. The ground-state energy of the mixed stacks has three minima as a function of the dimerization displacement, i.e., the N and the degenerate IA and IB states. The three states may be described by the spin-1 Ising variable  $p_{i,j} = 0, \pm 1$  on the  $i$ th dimer inside the  $j$ th stack.<sup>2,3,8</sup> The charge transfer energy ( $\Delta$ ), the intra- (with subscript  $\parallel$ ) and inter- (with subscript  $\perp$ ) stack dipolar ( $J$ ) and non-polar ( $K$ ) interactions, and the coupling with the electric field ( $E$ ) are described by the quasi one-dimensional (Q1D) Blume-Emery-Griffith (BEG) model,<sup>10</sup>  $\mathcal{H} = \mathcal{H}_{\parallel} + \mathcal{H}_{\perp}$ , where

$$\mathcal{H}_{\parallel} = - \sum_{i,j} [J_{\parallel} p_{i,j} p_{i+1,j} + K_{\parallel} p_{i,j}^2 p_{i+1,j}^2 - \Delta p_{i,j}^2 - E p_{i,j}], \quad (1)$$

$$\mathcal{H}_{\perp} = - \sum_{i,j} [J_{\perp} p_{i,j} p_{i,j+1} + K_{\perp} p_{i,j}^2 p_{i,j+1}^2]. \quad (2)$$

The intra-stack dipolar interaction  $J_{\parallel}$  is caused by coupling between the charge transfer and the lattice distortion,<sup>8</sup> while the inter-stack dipolar interaction is regarded as a direct interaction between the induced dipoles on adjacent stacks. The intra-stack couplings are much stronger than the inter-stack couplings, and the electric dipoles are aligned along the stacks. The energy cost to create one  $D^+A^-$  pair is given in the limit of no molecular overlap by  $\Delta = I - A - \alpha V$ , where  $I$  and  $A$  denote the donor's ionization energy and the acceptor's affinity, respectively, and  $\alpha V$  denotes the Madelung energy.<sup>11</sup> Generally speaking, increasing pressure decreases the lattice spacing  $a$  and consequently in-

creases  $V$ . Therefore,  $\Delta$  decreases upon applying pressure.

We treat the Hamiltonian (2) by using the self-consistent chain mean-field theory<sup>12</sup>. Introducing the thermal averages,  $\eta = \langle p_{i,j} \rangle$  and  $c = \langle p_{i,j}^2 \rangle$ , we have the effective 1D BEG model,

$$\mathcal{H}_{\parallel}^{\text{eff}} = - \sum_i [J_{\parallel} p_i p_{i+1} + K_{\parallel} p_i^2 p_{i+1}^2 - \tilde{\Delta} p_i^2 - \tilde{E} p_i] + \frac{z_{\perp}}{2} N J_{\perp} \eta^2 + \frac{z_{\perp}}{2} N K_{\perp} c^2, \quad (3)$$

where  $\tilde{\Delta} = \Delta - z_{\perp} K_{\perp} c$  and  $\tilde{E} = E - z_{\perp} J_{\perp} \eta$ , with  $z_{\perp} = 2$  being the inter-stack coordination number. Treating  $\mathcal{H}_{\parallel}^{\text{eff}}$  exactly by the transfer matrix method, we obtain the free energy per site,

$$f_{\text{BEG}}(\eta, c, T) = -T \ln \lambda(\tilde{\Delta}, \tilde{E}, T) + J_{\perp} \eta^2 + K_{\perp} c^2, \quad (4)$$

where  $\lambda(\tilde{\Delta}, \tilde{E}, T)$  is the maximum eigenvalue of the transfer matrix for  $\mathcal{H}_{\parallel}^{\text{eff}}$ , given by

$$\mathbf{T} = \begin{pmatrix} e^{\beta(J_{\parallel} + K_{\parallel} - \tilde{\Delta} - \tilde{E})} & e^{-\beta(\tilde{\Delta} + \tilde{E})/2} & e^{\beta(-J_{\parallel} + K_{\parallel} - \tilde{\Delta})} \\ e^{-\beta(\tilde{\Delta} + \tilde{E})/2} & 1 & e^{-\beta(\tilde{\Delta} - \tilde{E})/2} \\ e^{\beta(-J_{\parallel} + K_{\parallel} - \tilde{\Delta})} & e^{-\beta(\tilde{\Delta} - \tilde{E})/2} & e^{\beta(J_{\parallel} + K_{\parallel} - \tilde{\Delta} + \tilde{E})} \end{pmatrix}, \quad (5)$$

with  $\beta = 1/T$ . Possible phase diagrams of the BEG model have been extensively studied through mean-field theories,<sup>10,13</sup> renormalization-group,<sup>14</sup> and transfer-matrix methods.<sup>15</sup> For the parameter regions relevant to the present case,  $J_{\parallel}$ ,  $J_{\perp}$ ,  $K_{\parallel}$ ,  $K_{\perp}$ , and  $\Delta$  are all positive, so that a solid-liquid-gas type phase diagram with proper slopes of transition lines is not obtained.

## III. INTERCHAIN ELECTROSTRICTION

Then, we consider the inter-stack lattice degrees of freedom that have not explicitly been taken into account in (2). It is well known that an electrostriction effect potentially converts a continuous transition to a discontinuous one, since this gives rise to an additional negative free-energy term that contains the forth power of the relevant order parameter.<sup>16</sup> In the present case, we phenomenologically introduce an additional free energy,

$$f_{\text{elst}}(c, y) = -\frac{c^2}{b_0 + y} + \frac{1}{2} k y^2, \quad (6)$$

where the first and second terms represent Coulomb attraction between the nearest neighbor stacks<sup>9</sup> and the elastic energy for the distortion in the inter-stack direction. Note that  $f_{\text{elst}}(c, 0)$  has already been absorbed into  $K_{\perp}$ . The lattice constant without distortion is  $b_0$ , and  $y$  denotes the distortion. By minimizing  $f_{\text{elst}}(c, y)$  with respect to  $y$ , we obtain the optimized lattice constant,

$$b(T) = b_0 + y(T) \sim b_0 - 2\varepsilon_{\text{elst}} b_0^2 c^2, \quad (7)$$

where  $\varepsilon_{\text{elst}} = 1/(2kb_0^4)$  is a small constant. We thus have the energy gain due to the lattice distortion,

$$f_{\text{elst}}(c, T) \sim -\varepsilon_{\text{elst}}c^4. \quad (8)$$

Now, solving the self-consistent equations is reduced to searching  $(c, \eta)$  that gives the absolute minimum of the total free energy,  $f(\eta, c, T) = f_{\text{BEG}}(\eta, c, T) + f_{\text{elst}}(c, T)$ . The ionic phase is characterized by the ionicity condensation  $c = 1$ , while the ferroelectric phase is characterized by  $\eta \neq 0$ .

Note that, in the present scheme, any phase with  $c \neq 1$  is regarded as “neutral” and that the neutral phase has always  $\eta = 0$ . In the BEG model, because of three states  $p_{i,j} = 0, \pm 1$ ,  $c$  approaches the universal constant  $c = 2/3$  in the high temperature limit, where the entropy term dominates the internal energy term. Therefore, in the parameter region where  $c$  continuously increases upon decreasing temperature, we have  $2/3 < c \leq 1$ . In the experiments,<sup>1</sup> the ionicity continuously increases upon decreasing temperature and jumps from  $c \sim 0.3$  to  $c \sim 0.6$  at the NIT. Thus, concerning the quantitative magnitude of the ionicity, there arises a difference between the experimental result and the present analysis. This apparent difference comes from the fact that we mapped the intra-stack CT transfer and the DA dimerization onto the simple spin-1 Ising variables. Therefore, we should regard the difference as an artifact of the classical BEG model.

#### IV. NUMERICAL RESULTS AND PHASE DIAGRAM

From now on, we set  $J_{\parallel} = 1$  as an energy unit and the electric field  $E$  is set to be zero. In Fig. 1, we show the temperature dependence of  $c$  and  $\eta$  for various magnitudes of  $\Delta$  with  $K_{\parallel} = 0.4$ ,  $K_{\perp} = 0.06$ ,  $J_{\perp} = 0.03$ , and  $\varepsilon_{\text{elst}} = 0.0095$ . We introduce the condensation temperature  $T_{\text{cond}}$  and the crystallization temperature  $T_{\text{cryst}}$ . The ionicity jumps into  $c = 1$  at  $T_{\text{cond}}$ , while the ferroelectric order parameter acquires a finite magnitude  $\eta \neq 0$  at  $T_{\text{cryst}}$ . The ground state becomes ionic for  $\Delta < 1.49$ . Both  $c$  and  $\eta$  exhibits a discontinuous change at the same transition temperature (the sublimation temperature) for  $1.42 < \Delta < 1.49$ . That is to say,  $T_{\text{cond}} = T_{\text{cryst}}$ . For  $\Delta < 1.42$ , there appears a region,  $T_{\text{cryst}} < T < T_{\text{cond}}$ , where the system is ionic but still paraelectric. This region is identified with the  $I_{\text{para}}$  phase that is observed in TTF-CA under pressure. The point ( $\Delta_t = 1.42, T_t = 0.45$ ) is identified with the *triple point* (indicated by “TP” in Fig. 5). For  $\Delta < 1.42$ ,  $c$  still exhibits a discontinuous change at  $T_{\text{cond}}$ , but  $\eta$  continuously evolves at  $T_{\text{cryst}}$ , as shown in Fig. 1(c). The discontinuity jump of  $c$  becomes smaller and seems to vanish, as  $\Delta$  decreases, as shown in Fig. 1(d). We stress that this discontinuity is a direct consequence of the weak but finite electrostriction effect. Without the electrostriction, as  $\Delta$  decreases,  $T_{\text{cond}}$  and  $T_{\text{cryst}}$  continue to coincide with each

other, and the transition simply changes from discontinuous to continuous at some critical value of  $\Delta$ .<sup>10,13,14,15</sup>

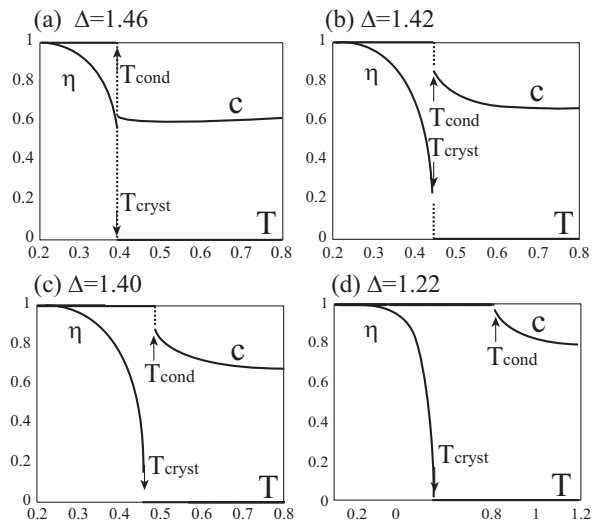


FIG. 1: Temperature dependence of  $c$  and  $\eta$  for various magnitudes of  $\Delta$  with  $K_{\parallel} = 0.4$ ,  $K_{\perp} = 0.06$ ,  $J_{\perp} = 0.03$ , and  $\varepsilon_{\text{elst}} = 0.0095$ . The condensation and crystallization temperature,  $T_{\text{cond}}$  and  $T_{\text{cryst}}$ , respectively, are indicated. Locations of the  $\Delta$  values in (a)-(d) are indicated in the phase diagram of Fig. 5.

As clearly seen from (7), about 0.5% discontinuous contraction of the inter-stack lattice constant (unit cell parameter  $b$ ) is accompanied by the discontinuous jump of the ionicity. In Fig. 2, setting  $b_0$  as a length unit, we show the temperature dependence of the unit cell parameter  $b$  given by (7), using the same parameter set as that in Fig. 1. Although the magnitude of the discontinuous contraction depends on the parameter choice of  $\varepsilon_{\text{elst}}$  and  $b_0$ , the qualitative nature ( $b$  jumps at  $T_{\text{cond}}$ ) does not change.

To see the discontinuity of the ionicity more closely, we show in Fig. 3 the  $\Delta$  dependence of the discontinuity at the condensation temperature,  $\Delta c$ . It is clearly seen that  $\Delta c$  decreases as  $\Delta$  decreases and eventually reaches zero at  $\Delta = 1.25$ . For  $\Delta < 1.25$ , the condensation occurs without ionicity jump. Then, the lattice contraction at  $T_{\text{cond}}$  also becomes continuous. Therefore,  $\Delta = 1.25$  with the corresponding  $T_{\text{cond}} = 0.76$  is identified with a *critical point* (indicated by “CP” in Fig. 5). This result is well consistent with the experimental fact that the ionicity jump finishes at the critical point.<sup>2</sup>

The dielectric constant is given by  $\varepsilon = 1 + 4\pi\alpha$ , where the uniform polarizability is  $\alpha = \frac{1}{T} \sum_{i,j} \sum_{l,m} [\langle p_{i,j} p_{l,m} \rangle - \langle p_{i,j} \rangle \langle p_{l,m} \rangle] = (c - \eta^2)/T$ . In Fig. 4, we show the temperature dependence of  $\alpha$  for various magnitudes of  $\Delta$ . It is seen that along the  $N$ - $I_{\text{ferro}}$  boundary, the polarizability exhibits a sharp single cusp at  $T_{\text{cond}} = T_{\text{cryst}}$ . For  $\Delta_c < \Delta < \Delta_t$ , a discontinuous jump occurs at  $T = T_{\text{cond}}$  and a cusp at  $T = T_{\text{cryst}}$ . The discontinuity at  $T = T_{\text{cond}}$  finishes at  $\Delta = \Delta_c$ .

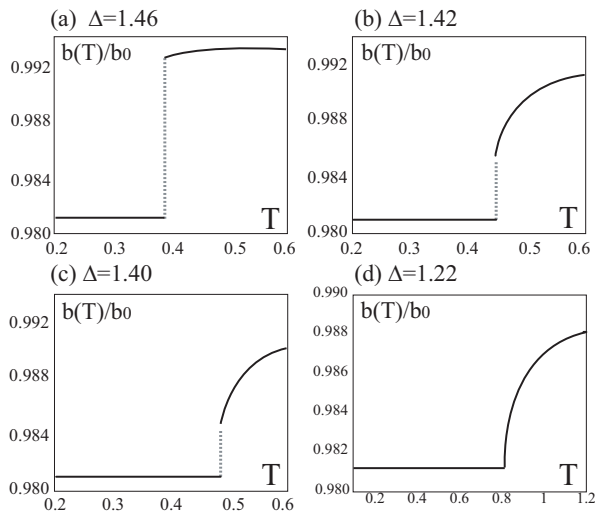


FIG. 2: Temperature dependence of the unit cell parameter  $b$ ,  $b(T)$ . Locations of the  $\Delta$  values in (a)-(d) are indicated in the phase diagram of Fig. 5.

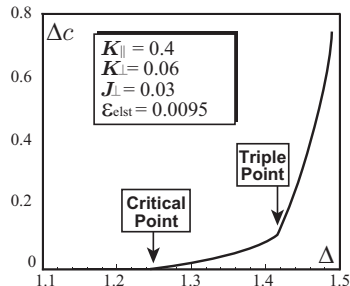


FIG. 3: Temperature dependence of the discontinuity of the ionicity,  $\Delta c$ .

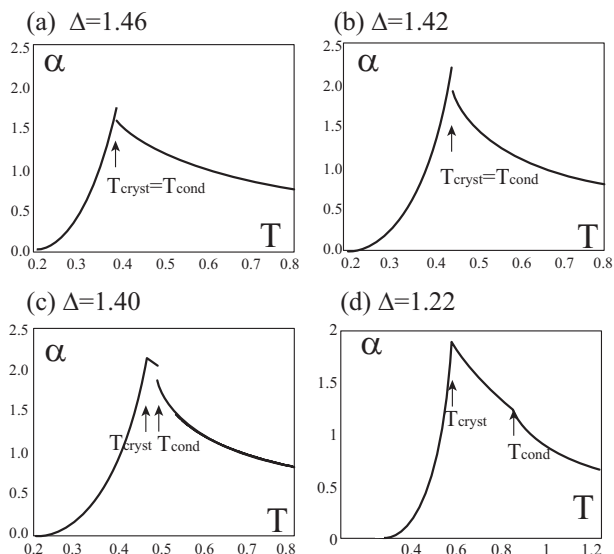


FIG. 4: Temperature dependence of the polarizability,  $\alpha$ . Locations of the  $\Delta$  values in (a)-(d) are indicated in the phase diagram of Fig. 5.

In Fig. 5, we show the phase diagram of the system for  $K_{\parallel} = 0.4$ ,  $K_{\perp} = 0.06$ ,  $J_{\perp} = 0.03$ , and  $\epsilon_{\text{elst}} = 0.0095$ . Regarding the decreasing  $\Delta$  as increasing pressure, this phase diagram is consistent with the experimentally found, pressure-temperature phase diagram of TTF-CA.<sup>2</sup> The triple point, the critical point, and the observed inter-stack lattice contraction are reproduced. For simplicity, we here ignored the change of  $\Delta$  due to thermal lattice contraction. Exactly speaking, to convert our  $\Delta$ - $T$  phase diagram to a  $P$ - $T$  diagram, we need to take account of the temperature dependence of  $\Delta$ ,  $\Delta(T)$ . By appropriately treating  $\Delta(T)$ , we may obtain the corresponding  $P$ - $T$  phase diagram satisfying the Clausius-Clapeyron relation. We stress that, even when we take this simple view, a qualitative nature of the phase diagram is not changed. Identifying the triple point  $(\Delta_t, T_t) = (1.42, 0.45)$  with the experimentally obtained one  $(P_t, T_t) \sim (500\text{MPa}, 210\text{K})$ , we see that our parameter choice here corresponds to  $K_{\perp} = 28\text{K}$  and  $J_{\perp} = 14\text{K}$ .

Lajzerowicz and Sivardi re<sup>17</sup> extensively developed a mean-field analysis of the BEG model and obtained liquid-gas-solid like phase diagrams on the  $P$ - $T$  plane. However, they considered a lattice gas analogue of a simple fluid, where the physical pressure of the lattice gas is simply given by  $-f$ , with  $f$  being the Helmholtz free energy per volume. In the present context, the pressure of the spin system has no physical meaning and the phase diagram obtained by Lajzerowicz and Sivardi re cannot be applied to TTF-CA.

## V. CONCLUDING REMARKS

In this paper, we showed that the inter-stack electrostriction causes the  $-c^4$  term with a small coefficient and makes the phase diagram rich. We thus conclude that the inter-stack polar interaction together with the inter-stack electrostriction drives the discontinuous inter-stack lattice contraction and the multicritical behavior observed in TTF-CA.<sup>2,3</sup> Our considerations are limited to classical models, i.e., we considered classical *effective* models, where all the microscopic (electronic or phonon) degrees of freedom are implicitly integrated out. To obtain the truly microscopic mechanism behind the multicriticality, we need to get back to such a microscopic Hamiltonian as an extended Peierls-Hubbard model.<sup>18</sup> We would keep this issue for future study.

This work was partly supported by a Grant-in-Aid for Scientific Research (C) from Japan Society for the Promotion of Science. TL wishes to acknowledge hospitality at the Institute for Molecular Sciences, Okazaki, and thank colleagues for creating a pleasant and stimulating environment there.

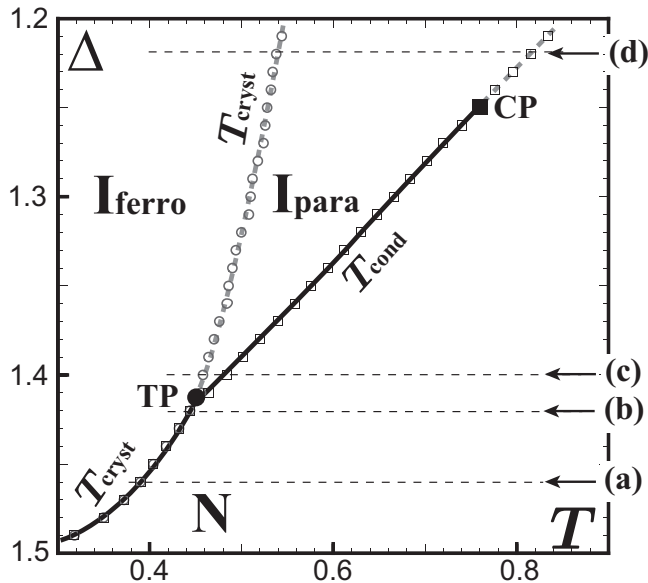


FIG. 5: Phase diagram for  $K_{\parallel} = 0.4$ ,  $K_{\perp} = 0.06$ ,  $J_{\perp} = 0.03$ , and  $\epsilon_{\text{elst}} = 0.0095$ . The solid and dashed lines represent discontinuous and continuous transitions, respectively. **TP** and **CP** represent the triple point and the critical point, respectively. Locations of the  $\Delta$  values used in (a)-(d) of Figs. 1, 2, and 4 are indicated by the horizontal arrows.

- 
- <sup>1</sup> J. B. Torrance, J. E. Vazquez, J. J. Mayerle, and V. Y. Lee, Phys. Rev. Lett. **46**, 253 (1981).
  - <sup>2</sup> M. H. Lemée-Cailleau, M. Le Cointe, H. Cailleau, T. Luty, F. Moussa, J. Roos, D. Brinkmann, B. Toudic, C. Ayache, and N. Karl, Phys. Rev. Lett. **79**, 1690 (1997).
  - <sup>3</sup> T. Luty, H. Cailleau, S. Koshihara, E. Collet, M. Takeda, M-H. Lemée-Cailleau, M. Buron-Le Cointe, N. Nagaosa, Y. Tokura, E. Zienkiewicz, and B. Ouladdiaf, Europhys. Lett. **59**, 619 (2002).
  - <sup>4</sup> S. Koshihara, Y. Tokura, K. Takeda, T. Koda, Phys. Rev. Lett. **68**, 1148 (1992).
  - <sup>5</sup> E. Collet, M. H. Lemée-Cailleau, M. Buron-Le Cointe, H. Cailleau, M. Wulff, T. Luty, S. Koshihara, M. Meyer, L. Toupet, P. Rabiller and S. Techert, Science, **300**, 612 (2003).
  - <sup>6</sup> T. Iizuka-Sakano and Y. Toyozawa, J. Phys. Soc. Jpn. **65**, 671 (1996).
  - <sup>7</sup> N. Nagaosa, J. Phys. Soc. Jpn. **55**, 3488 (1986).
  - <sup>8</sup> T. Luty in *Relaxatoin of Excited States and Photo-Induced Structural Phase Transitions*, edited by K. Nasu, Springer Series in Solid-State Sciences **124** (Springer-Verlag, 1996) p. 142.
  - <sup>9</sup> T. Kawamoto, T. Iizuka-Sakano, Y. Shimoi, and S. Abe, Phys. Rev. B **64**, 205107 (2001).
  - <sup>10</sup> M. Blume, V. J. Emery, and R. B. Griffiths, Phys. Rev. A **4**, 1071 (1971).
  - <sup>11</sup> H. M. McConnell, B. M. Hoffman, and R. M. Metzger, Proc. Natl. Acad. Sci. U.S.A. **53**, 46 (1965).
  - <sup>12</sup> D. J. Scalapino, Y. Imry, and P. Pincus, Phys. Rev. B **11**, 2042 (1975).
  - <sup>13</sup> W. Hoston, A. N. Berker, Phys. Rev. Lett. **67**, 1027 (1991).
  - <sup>14</sup> A. N. Berker and M. Wortis, Phys. Rev. B **14**, 4946 (1976)
  - <sup>15</sup> E. Albayrak and M. Keskin, J. Mag. Mag. Mater. **213**, 201 (2000).
  - <sup>16</sup> See, for example, P. W. Anderson, *Basic Notions of Condensed Matter Physics*, (Addison-Wesley, 1984), Section 2 C.
  - <sup>17</sup> J. Lajzerowicz and J. Sivardière, Phys. Rev. A **11**, 2079 (1975).
  - <sup>18</sup> N. Miyashita, M. Kuwabara, and K. Yonemitsu, cond-mat/0211487 (unpublished), J. Phys. Soc. Jpn. (in press).